Optical and Quantum Electronics (2024) 56:504
https://doi.org/10.1007/s11082-023-06036-5

# Dynamic simulation of traveling wave solutions for the differential-difference Burgers' equation utilizing a generalized exponential rational function approach

**Mostafa Eslami[1] · Samira Heidari[1] · Sajjad A. Jedi Abduridha[2] · Yasin Asghari[1]**

Received: 2 October 2023 / Accepted: 3 December 2023 / Published online: 30 January 2024


**Abstract**
This article aims to study the generalized exponential rational function method to solve the differential-difference Burgers' equation. Our approach is an efficient method for solving nonlinear partial differential equations, and it can be used for a specific type of nonlinear differential-difference equations. To recognize diverse singular soliton and multi-soliton wave structures, we displayed the 3-D and contour graphs associated with the solutions.

**Keywords** Differential-difference Burgers' equation · Traveling wave solutions · Generalized exponential rational function approach

## 1 Introduction

Despite the difficulty of studying nonlinear differential-difference equations (NDDEs), this class of equations has always been considered one of the most essential tools for researchers to describe various models in different fields of science (Parand and Delkhosh 2017; Houwe etal. 2020; Rasheed etal. 2023). The importance of NDDEs has dramatically increased with the development of new concepts, causing classical methods to be incapable of solving some of these new types of equations. The role of NPDEs and NDDEs is evident in describing many biological phenomena (Wang and Wen 2018; Parand etal. 2017b, c; Akram et al. 2023).

✉ Mostafa Eslami
Mostafa.eslami@umz.ac.ir

Samira Heidari
samira_heidari178@yahoo.com

Sajjad A. Jedi Abduridha
sajjada.jedi@uokufa.edu.iq

Yasin Asghari
y.asghari01@umail.umz.ac.ir

[1] Faculty of Mathematical Sciences, University of Mazandaran, Babolsar, Iran

[2] Department of Mathematics, Faculty of Basic Education, University of Kufa, Najaf, Iraq

To achieve exact solutions in solving NPDEs and NDDEs, numerous established analytical techniques have been effective, for instance: the He-Elzaki transform method (Modanli etal. 2023), extended $(G'/G^2)$-expansion method (Akram and Zainab 2020), residual Power seriesn method (Abdulazeez et al. 2023; Tariq etal. 2023; Modanli etal. 2021), homotopy analysis approach (Abdulazeez etal. 2022; Sadaf and Akram 2021), the extended Sinh-Gordon equation expansion technique (Akram et al. 2022; Sadaf etal. 2022), the explicit finite difference method (Abdulazeez and Modanli 2022), the improved $\tan(\Psi(\zeta)/2)$-expansion method (Akram etal. 2022), the modified simple equation approach (Akram et al. 2023), modified auxiliary equation approach (Sadaf etal. 2023), generalized Kudryashov method (Akram etal. 2023), the generalized Pseudospectral approach (Delkhosh and Parand 2019; Delkhosh and Cheraghian 2022), etc.

This research aims to bring forth exact solutions using a recently developed generalized exponential function method (GERFM), This method is one of the effective methods for calculating exact wave solutions, which is used in the present article to solve the DDBE.

This method was already introduced by Ghanbari in 2018 (Ghanbari and Inc 2018), and after that year, he and other researchers have repeatedly used it for partial differential equations. For instance, Ghanbari and Kuo (2019) found exact wave solutions for the variable-coefficient (1 + 1)-dimensional Benjamin-Bona-Mahony and (2 + 1)-dimensional asymmetric Nizhnik-Novikov-Veselov equations by means of the GERFM. Also, Ghanbari etal. (2020) presented the generalized exponential function method to a novel extension of the nonlinear Schrödinger equation. Tarla etal. (2022) investigates the propagation of solitons in the Hamiltonian amplitude equation via GERFM.

The differential-difference Burgers' equation (DDBE) that incorporates discrete terms along with continuous terms. This equation is used to model systems where both continuous and discrete processes play a role in the evolution of the variables. The differential-difference Burgers' equation (DDBE) has applications in various fields, including hydrodynamics, fluid dynamics, nonlinear acoustic waves, mathematical physics, biological systems, numerical simulations, and materials science (Mohanty et al. 2022).

The general form of such an equation looks like this:

$$\frac{\mathrm{d}\mathfrak{u}_k(t)}{\mathrm{d}t} = \big(1 + \mathfrak{u}_k(t)\big)\big(\mathfrak{u}_{k+1}(t) - \mathfrak{u}_k(t)\big). \tag{1}$$

Where $\mathfrak{u}_k(t) = \mathfrak{u}(k,t)$, $k \in \mathbb{Z}$, This equation in 2010 by Aslan (2012) was solved using the discrete $(G'/G)$-expansion method.

The generality of GERFM is described in Sect. 2, where we address the requirements of this approach and the categorization of the solutions. Section 3 presents the GERFM for solving the differential-difference Burgers' equation and the associated traveling wave solutions utilizing 3D and contour diagrams. In the final part, we deliver a summary of our findings.

## 2 Procedure analysis

In this section, the GERFM method is briefly explained. Consider the differential-difference equation in the following form:

$$\begin{aligned}&\mathcal{N}(\mathfrak{u}_{m+p_1}(t),\dots,\mathfrak{u}_{m+p_k}(t),\dots,\mathfrak{u}^{\alpha}{}_{m+p_1}(t),\dots,\\&\mathfrak{u}^{\alpha}{}_{m+p_k}(t),\dots,\mathfrak{u}^{(r\alpha)}{}_{m+p_1}(t),\dots,\mathfrak{u}^{(r\alpha)}{}_{m+p_k}(t))=0,\end{aligned}\tag{2}$$

Using the following traveling wave transform

$$\begin{aligned}&\mathfrak{u}_{k+p_s}(t)=\mathfrak{U}_k(\zeta_k),\quad s=1,2,\dots,k,\\&\zeta_k=\mathrm{d}k+ct+\zeta_0.\end{aligned}\tag{3}$$

Where $d$ and $c$ are constants to be determined later, then Eq. (2) reduces to an ODE of the following form:

$$\begin{aligned}&\mathcal{Q}(\mathfrak{U}_{m+p_1}(\zeta_n),\dots,\mathfrak{U}_{m+p_k}(\zeta_n),\dots,\mathfrak{U}'{}_{m+p_1}(\zeta_n),\dots,\\&\mathfrak{U}'{}_{m+p_k}(\zeta_n),\dots,\mathfrak{U}^{(r)}{}_{m+p_1}(\zeta_n),\dots,\mathfrak{U}^{(r)}{}_{m+p_k}(\zeta_n))=0.\end{aligned}\tag{4}$$

This technique is built using a hypothetical solution that can be displayed as follows:

$$\mathcal{Y}(\zeta_k)=\mathcal{V}_0+\sum_{\mathfrak{i}=1}^{a_0}\mathcal{V}_{\mathfrak{i}}\mathbb{L}^{\mathfrak{i}}(\zeta_k)+\sum_{\mathfrak{i}=1}^{a_0}\frac{\mathcal{Z}_{\mathfrak{i}}}{\mathbb{L}^{\mathfrak{i}}(\zeta_k)}.\tag{5}$$

$$\mathbb{L}(\zeta_k)=\frac{r_1\exp(\gamma_1\zeta_k)+r_2\exp(\gamma_2\zeta_k)}{r_3\exp(\gamma_3\zeta_k)+r_4\exp(\gamma_4\zeta_k)}.\tag{6}$$

In Eq. (5), $\mathcal{V}_0,\mathcal{V}_{\mathfrak{i}},\mathcal{Z}_{\mathfrak{i}}(1\le\mathfrak{i}\le a_0)$, and in Eq. (6) $r_{\mathfrak{i}},\gamma_{\mathfrak{i}},(1\le\mathfrak{i}\le 4)$, Recall that we use the balance rules to determine the positive integer $a_0$.

Now, in this research, we show that the following relations can be considered in Eq. (4) as follows:

$$\begin{aligned}&\mathfrak{u}_{k+1}(t)=\mathfrak{U}(\zeta_{k+1})=\mathfrak{U}(\zeta_k+d),\\&\mathfrak{u}_{k-1}(t)=\mathfrak{U}(\zeta_{k-1})=\mathfrak{U}(\zeta_k-d).\end{aligned}\tag{7}$$

By inserting Eq. (5) into Eq. (4), we obtain a polynomial, which indicates that the analytical solutions for Eq. (2) are obtained.

## 3 Applications of GERFM for the DDBE

To solve Eq. (1), using the method of GERFM, as explained in the previous section, we first apply the transformation $\mathfrak{u}_k(t)=\mathfrak{U}(\zeta_k)$, $\zeta_k=\mathrm{d}k+ct+\zeta_0$, where $d$ and $c$ are constants to be determined, and $\zeta_0$ is an arbitrary phase constant, to arrive at the following ordinary differential equation:

$$c\mathfrak{U}'(\zeta_k)=(1+\mathfrak{U}(\zeta_k))(\mathfrak{U}_{k+1}(\zeta_k)-\mathfrak{U}(\zeta_k)).\tag{8}$$

According to the method explained in the previous section, balancing the highest-order linear term with the highest nonlinear term in Eq. (8) yields $a_0=1$. Therefore, we will have the solution of the equation in the following hypothetical form:

$$\mathcal{Y}(\zeta_k) = \mathcal{V}_0 + \mathcal{V}_1 \mathbb{L}(\zeta_k) + \frac{\mathcal{Z}_1}{\mathbb{L}(\zeta_k)}. \tag{9}$$

Where the constant coefficients of $\mathcal{V}_0$, $\mathcal{V}_1$, $\mathcal{Z}_1$ are determined in the next step, and $\mathbb{L}(\zeta_k)$ is obtained according to Eq. (5).

**Category I:** catching $[r_1\ r_2\ r_3\ r_4] = [-1\ 1\ 1\ 1]$ and $[\gamma_1\ \gamma_1\ \gamma_1\ \gamma_1] = [1\ -1\ 1\ -1]$ in Eq. (5) render:

$$\mathbb{L}(\zeta_k) = -\tanh(\zeta_k). \tag{10}$$

By putting Eq. (9) into Eq. (8) and collecting coefficients of $\mathbb{L}^i(\zeta_k)$ for $i = 0, 1, 2...$ and setting them to zero, we derive a system of algebraic equations. By solving this system using MAPLE software, we can determine the unknown parameters. Therefore, the many various anthologies are obtained as follows:

**Set 1:**

$$c = -\mathcal{V}_1, \quad \mathcal{V}_0 = -(2\mathcal{V}_1 + 1)tanh(2d), \quad \mathcal{Z}_1 = \mathcal{V}_1.$$

Where $d, \mathcal{V}_1$ are constant. By substituting the values of the above obtained parameters into Eq. (8), the following traveling wave solution is obtained:

$$\mathcal{Y}(\zeta_k) = -(2\mathcal{V}_1 + 1)tanh(2d) - \mathcal{V}_1 tanh(\zeta_k) - \frac{\mathcal{V}_1}{tanh(\zeta_k)}. \tag{11}$$

Where $\zeta_k = kd - \mathcal{V}_1 t + \zeta_0$.

The graphical diagrams related to this traveling wave solution Eq. (11) is presented in Fig. 1.

**Set 2:**

$$c = -\mathcal{V}_1, \quad \mathcal{V}_0 = -1 - \mathcal{V}_1 coth(d), \quad \mathcal{Z}_1 = 0.$$

Where $d, \mathcal{V}_1$ are constant. By substituting the values of the above obtained parameters into Eq. (8), the following traveling wave solution is obtained:

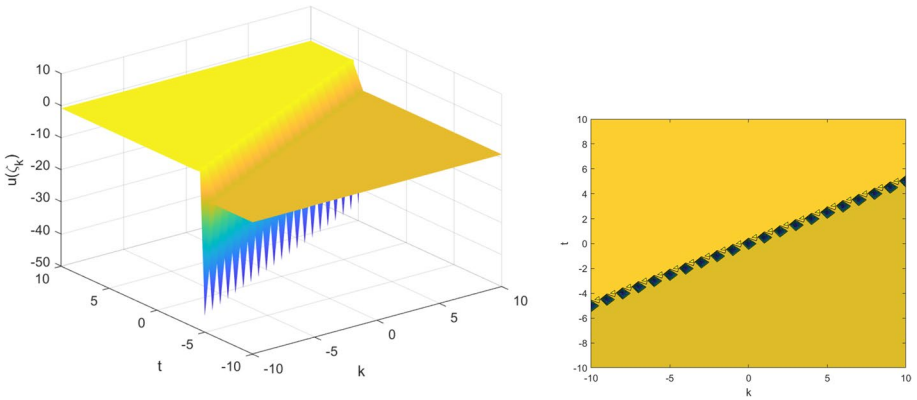


**Fig. 1** The graphical 3D and contour diagrams related to the solution of Eq. (11) with parameters $d = 1, V_1 = 2, \zeta_0 = 0.05$

$$\mathcal{Y}(\zeta_k) = -1 - \mathcal{V}_1 coth(d) - \mathcal{V}_1 tanh(\zeta_k). \tag{12}$$

Where $\zeta_k = kd - \mathcal{V}_1 t + \zeta_0$.

The graphical diagrams related to this traveling wave solution Eq. (12) is presented in Fig. 2.

**Set 3:**

$$c = -\mathcal{Z}_1, \quad \mathcal{V}_0 = -1 - \mathcal{Z}_1 coth(d), \quad \mathcal{V}_1 = 0.$$

Where $d, \mathcal{Z}_1$ are constant. By substituting the values of the above obtained parameters into Eq. (8), the following traveling wave solution is obtained:

$$\mathcal{Y}(\zeta_k) = -1 - \mathcal{Z}_1 coth(d) - \frac{\mathcal{Z}_1}{tanh(\zeta_k)}. \tag{13}$$

Where $\zeta_k = kd - \mathcal{Z}_1 t + \zeta_0$.

The graphical diagrams related to this traveling wave solution Eq. (13) is presented in Fig. 3.

**Category II:** catching $\left[r_1\ r_2\ r_3\ r_4\right] = [i\ -i\ 1\ 1]$ and $\left[\gamma_1\ \gamma_1\ \gamma_1\ \gamma_1\right] = [-i\ i\ -i\ i]$ in Eq. (5) render:

$$\mathbb{L}(\zeta_k) = -tan(\zeta_k). \tag{14}$$

the many various anthologies are obtained as follows:

**Set 1:**

$$c = \mathcal{V}_1, \quad \mathcal{V}_0 = \frac{-\left(\tan^2(d)\right)\mathcal{V}_1 - \tan(d) + \mathcal{V}_1}{\tan(d)}, \quad \mathcal{Z}_1 = -\mathcal{V}_1.$$

Where $d, \mathcal{V}_1$ are constant. By substituting the values of the above obtained parameters into Eq. (8), the following traveling wave solution is obtained:

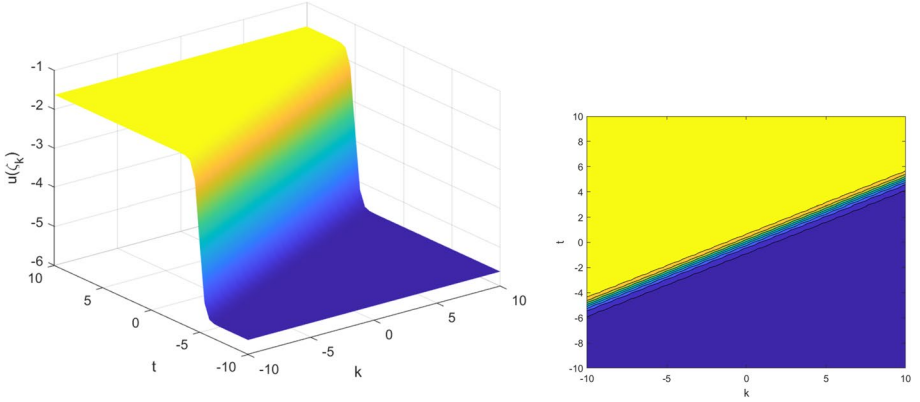


**Fig. 2** The graphical 3D and contour diagrams related to the solution of Eq. (12) with parameters $d = 1, V_1 = 2, \zeta_0 = 0.05$

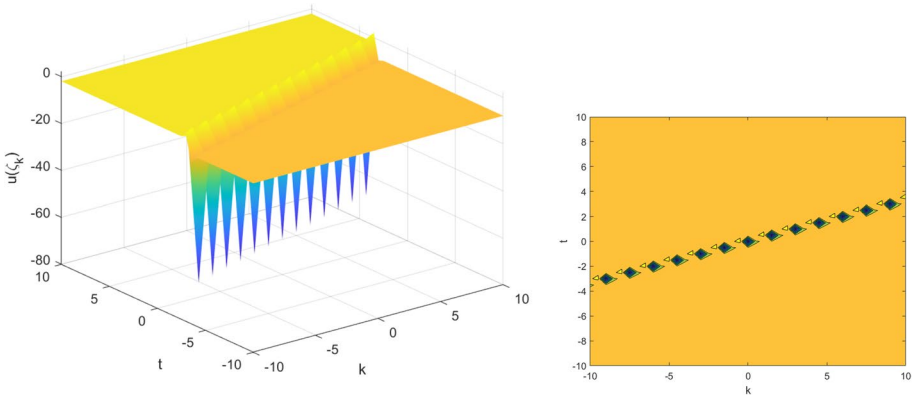


**Fig. 3** The graphical 3D and contour diagrams related to the solution of Eq. (13) with parameters $d = 1, Z_1 = 3, \zeta_0 = 0.05$

$$\mathcal{Y}(\zeta_k) = \frac{-\left(\tan^2(d)\right)\mathcal{V}_1 - \tan(d) + \mathcal{V}_1}{\tan(d)} - \mathcal{V}_1 tan(\zeta_k) + \frac{\mathcal{V}_1}{tan(\zeta_k)}. \tag{15}$$

Where $\zeta_k = kd + \mathcal{V}_1 t + \zeta_0$.

The graphical diagrams related to this traveling wave solution Eq. (15) is presented in Fig. 4.

**Set 2:**

$$c = \tan(d)\left(\mathcal{V}_0 + 1\right), \quad \mathcal{V}_1 = \tan(d)\left(\mathcal{V}_0 + 1\right), \quad \mathcal{Z}_1 = 0.$$

Where $d, \mathcal{V}_0$ are constant. By substituting the values of the above obtained parameters into Eq. (8), the following traveling wave solution is obtained:

$$\mathcal{Y}(\zeta_k) = \mathcal{V}_0 - \tan(d)\left(\mathcal{V}_0 + 1\right) tan(\zeta_k). \tag{16}$$

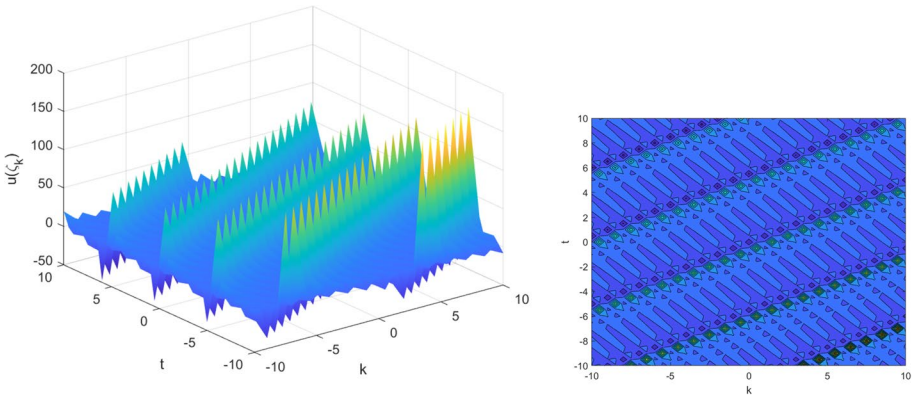


**Fig. 4** The graphical 3D and contour diagrams related to the solution of Eq. (15) with parameters $d = 1, V_1 = -2, \zeta_0 = 0.05$

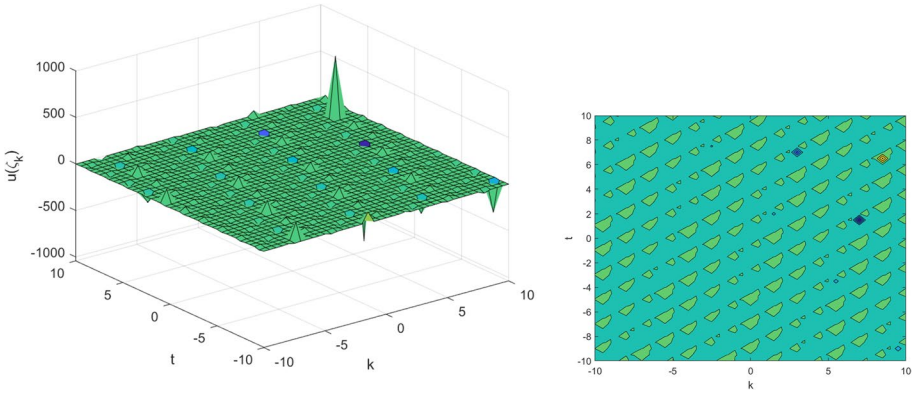


**Fig. 5** The graphical 3D and contour diagrams related to the solution of Eq. (16) with parameters $d = 1, V_0 = -2, \zeta_0 = 0.05$

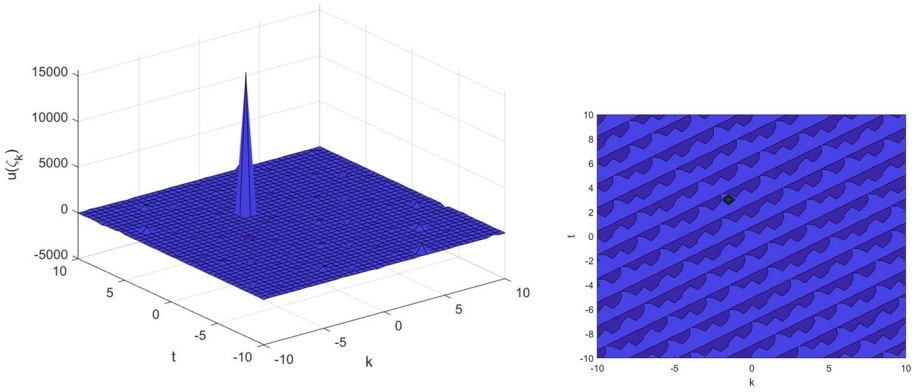


**Fig. 6** The graphical 3D and contour diagrams related to the solution of Eq. (17) with parameters $d = 1, V_0 = -2, \zeta_0 = 0.05$

Where $\zeta_k = kd + \tan(d)\big(\mathcal{V}_0 + 1\big)t + \zeta_0$.

The graphical diagrams related to this traveling wave solution Eq. (16) is presented in Fig. 5.

**Set 3:**

$$c = \tan(d)\big(\mathcal{V}_0 + 1\big), \quad \mathcal{V}_1 = 0, \quad \mathcal{Z}_1 = -\tan(d)\big(\mathcal{V}_0 + 1\big).$$

Where $d, \mathcal{V}_0$ are constant. By substituting the values of the above obtained parameters into Eq. (8), the following traveling wave solution is obtained:

$$\mathcal{Y}(\zeta_k) = \mathcal{V}_0 + \frac{\tan(d)\big(\mathcal{V}_0 + 1\big)}{tan(\zeta_k)}. \tag{17}$$

Where $\zeta_k = kd + \tan(d)\big(\mathcal{V}_0 + 1\big)t + \zeta_0$.

The graphical diagrams related to this traveling wave solution Eq. (17) is presented in Fig. 6.

**Category III:** catching $\left[r_1\ r_2\ r_3\ r_4\right] = [1\ 1\ -1\ 1]$ and $\left[\gamma_1\ \gamma_1\ \gamma_1\ \gamma_1\right] = [1\ -1\ 1\ -1]$ in Eq. (5) render:

$$\mathbb{L}\left(\zeta_k\right) = -coth(\zeta_k). \tag{18}$$

The many various anthologies are obtained as follows:

**Set 1:**

$$c = -\mathcal{V}_1, \quad \mathcal{V}_0 = -(2\mathcal{V}_1 + 1)tanh(2d), \quad \mathcal{Z}_1 = \mathcal{V}_1.$$

Where $d, \mathcal{V}_1$ are constant. By substituting the values of the above obtained parameters into Eq. (8), the following traveling wave solution is obtained:

$$\mathcal{Y}\left(\zeta_k\right) = -(2\mathcal{V}_1 + 1)tanh(2d) - \mathcal{V}_1 coth(\zeta_k) - \frac{\mathcal{V}_1}{coth(\zeta_k)}. \tag{19}$$

Where $\zeta_k = kd - \mathcal{V}_1 t + \zeta_0$.

The graphical diagrams related to this traveling wave solution Eq. (19) is presented in Fig. 7.

**Set 2:**

$$c = -\mathcal{V}_1, \quad \mathcal{V}_0 = -1 - \mathcal{V}_1 coth(d), \quad \mathcal{Z}_1 = 0.$$

Where $d, \mathcal{V}_1$ are constant. By substituting the values of the above obtained parameters into Eq. (8), the following traveling wave solution is obtained:

$$\mathcal{Y}\left(\zeta_k\right) = -1 - \mathcal{V}_1 coth(d) - \mathcal{V}_1 coth(\zeta_k). \tag{20}$$

Where $\zeta_k = kd - \mathcal{V}_1 t + \zeta_0$.

The graphical diagrams related to this traveling wave solution Eq. (20) is presented in Fig. 8.

**Set 3:**

$$c = -\mathcal{Z}_1, \quad \mathcal{V}_0 = -1 - \mathcal{Z}_1 coth(d), \quad \mathcal{V}_1 = 0.$$

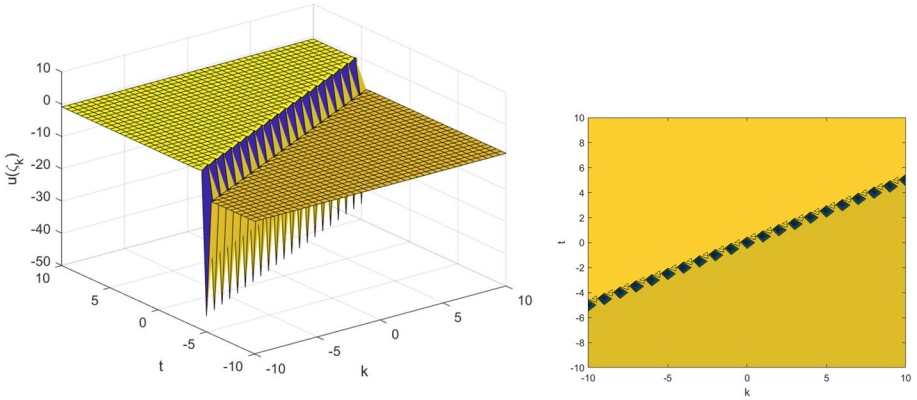


**Fig. 7** The graphical 3D and contour diagrams related to the solution of Eq. (19) with parameters $d = 1, V_1 = 2, \zeta_0 = 0.05$

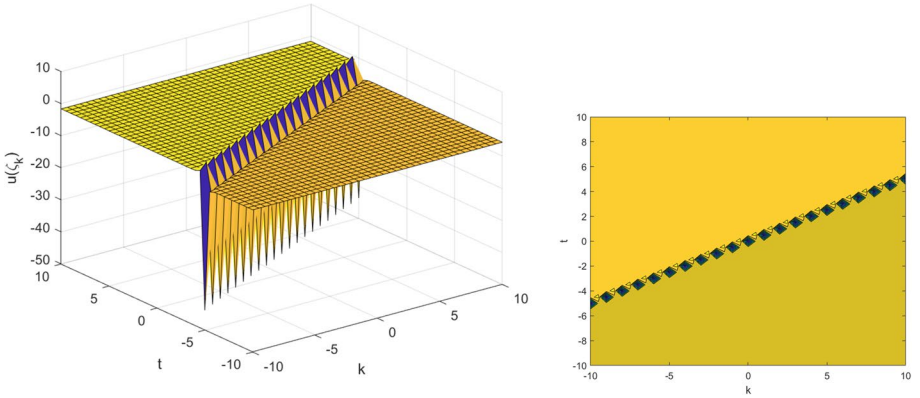


**Fig. 8** The graphical 3D and contour diagrams related to the solution of Eq. (20) with parameters $d = 1, V_1 = 2, \zeta_0 = 0.05$

Where $d, \mathcal{Z}_1$ are constant. By substituting the values of the above obtained parameters into Eq. (8), the following traveling wave solution is obtained:

$$\mathcal{Y}(\zeta_k) = -1 - \mathcal{Z}_1 coth(d) - \frac{\mathcal{Z}_1}{coth(\zeta_k)}. \tag{21}$$

Where $\zeta_k = kd - \mathcal{Z}_1 t + \zeta_0$.

The graphical diagrams related to this traveling wave solution Eq. (21) is presented in Fig. 9.

**Category IV:** catching $\left[r_1\ r_2\ r_3\ r_4\right] = [-1\ 0\ 1\ 1]$ and $\left[\gamma_1\ \gamma_1\ \gamma_1\ \gamma_1\right] = [0\ 0\ 0\ 1]$in Eq. (5) render:

$$\mathbb{L}(\zeta_k) = -\cot(\zeta_k). \tag{22}$$

The many various anthologies are obtained as follows:

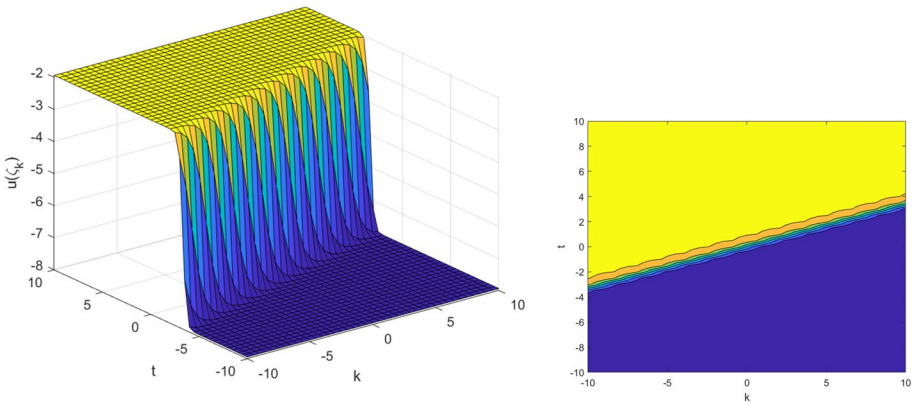


**Fig. 9** The graphical 3D and contour diagrams related to the solution of Eq. (21) with parameters $d = 1, Z_1 = 3, \zeta_0 = 0.05$

**Set 1:**

$$c = -\mathcal{V}_1, \quad \mathcal{V}_0 = \frac{\left(\tan^2(d)\right)\mathcal{V}_1 - \tan(d) - \mathcal{V}_1}{\tan(d)}, \quad \mathcal{Z}_1 = -\mathcal{V}_1.$$

Where $d, \mathcal{V}_1$ are constant. By substituting the values of the above obtained parameters into Eq. (8), the following traveling wave solution is obtained:

$$\mathcal{Y}(\zeta_k) = \frac{\left(\tan^2(d)\right)\mathcal{V}_1 - \tan(d) - \mathcal{V}_1}{\tan(d)} - \mathcal{V}_1 cot(\zeta_k) + \frac{\mathcal{V}_1}{cot(\zeta_k)}. \tag{23}$$

Where $\zeta_k = kd - \mathcal{V}_1 t + \zeta_0$.

The graphical diagrams related to this traveling wave solution Eq. (23) is presented in Fig. 10.

**Set 2:**

$$c = -\mathcal{V}_1, \quad \mathcal{V}_0 = -\mathcal{V}_1 cot(d) - 1, \quad \mathcal{Z}_1 = 0.$$

Where $d, \mathcal{V}_1$ are constant. By substituting the values of the above obtained parameters into Eq. (8), the following traveling wave solution is obtained:

$$\mathcal{Y}(\zeta_k) = -\mathcal{V}_1 cot(d) - 1 - \mathcal{V}_1 cot(\zeta_k). \tag{24}$$

Where $\zeta_k = kd - \mathcal{V}_1 t + \zeta_0$.

The graphical diagrams related to this traveling wave solution Eq. (24) is presented in Fig. 11.

**Set 3:**

$$c = \mathcal{Z}_1, \quad \mathcal{V}_0 = \mathcal{Z}_1 cot(d) - 1, \quad \mathcal{V}_1 = 0.$$

Where $d, \mathcal{Z}_1$ are constant. By substituting the values of the above obtained parameters into Eq. (8), the following traveling wave solution is obtained:

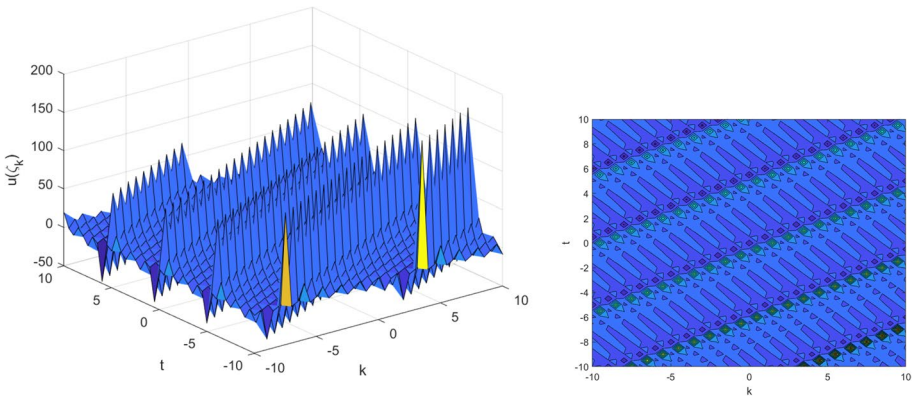


**Fig. 10** The graphical 3D and contour diagrams related to the solution of Eq. (23) with parameters $d = 1, V_1 = 2, \zeta_0 = 0.05$

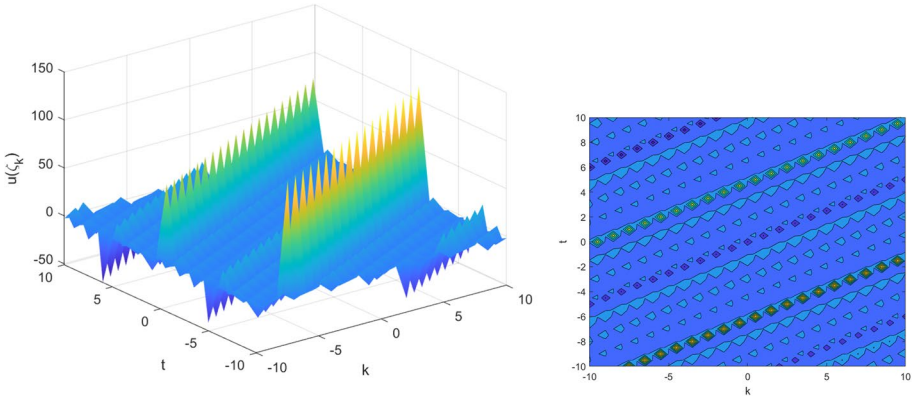


**Fig. 11** The graphical 3D and contour diagrams related to the solution of Eq. (24) with parameters $d = 1, V_1 = 2, \zeta_0 = 0.05$

$$\mathcal{Y}(\zeta_k) = \mathcal{Z}_1 cot(d) - 1 - \frac{\mathcal{Z}_1}{cot(\zeta_k)}. \tag{25}$$

Where $\zeta_k = kd + \mathcal{Z}_1 t + \zeta_0$.

The graphical diagrams related to this traveling wave solution Eq. (25) is presented in Fig. 12.

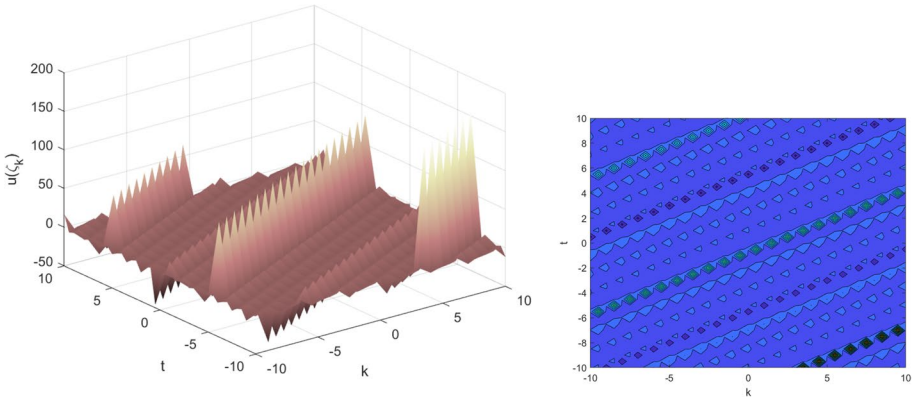


**Fig. 12** The graphical 3D and contour diagrams related to the solution of Eq. (25) with parameters $d = 1, Z_1 = 3, \zeta_0 = 0.05$

## 4 Conclusion

In this article, we obtained several solutions for the differential-difference Burgers' equation using generalized exponential functions, such as hyperbolic and trigonometric function solutions. Also, the singular soliton, multi-soliton, and kink-soliton solutions were obtained, each having a different form that is used to describe physical phenomena. We displayed the 3-D and contour graphs associated with the solutions. Based on the findings of this research, the proposed strategy offers promising solutions to this problem.

**Acknowledgment** This research was supported by a research grant from the University of Mazandaran.

**Author Contributions** SH and YA gave the first idea of investigation. The concept and modeling was done by ME The methodology, reviewing and editing has been done by SAJ

**Funding** The authors declare that no funds.

**Data availability** There is no data set used.

## Declarations

**Ethical approval** The authors declare that there is no animal studies in this work.

**Conflict of interest** The authors declare that they have no conflict of interest.

## References

Abdulazeez, S.T., Modanli, M.: Solutions of fractional order pseudo-hyperbolic telegraph partial differential equations using finite difference method. Alexandria Eng. J. **61**, 12443–12451 (2022)

Abdulazeez, S.T., Modanli, M., Husien, A.M.: Numerical scheme methods for solving nonlinear pseudo-hyperbolic partial differential equations. J. Appl. Math. Comput. Mech. **21**, 5–15 (2022)

Abdulazeez, S.T., Modanli, M., Husien, A.M.: Solutions to nonlinear pseudo hyperbolic partial differential equations with nonlocal conditions by using residual power series method. Sigma **41**(3), 488–492 (2023)

Akram, G., Arshed, S., Sadaf, M., Maqbool, M.: Comparison of fractional effects for phi-4 equation using beta and m-truncated derivatives. Opt. Quant. Electron. **55**(3), 282 (2023)

Akram, G., Sadaf, M., Arshed, S., Ejaz, U.: Travelling wave solutions and modulation instability analysis of the nonlinear Manakov-system. J. Taibah Univ. Sci. **17**, 12 (2023). https://doi.org/10.1080/16583655.2023.2201967

Akram, G., Sadaf, M., Arshed, S., Sabir, H.: Optical soliton solutions of fractional sasa-satsuma equation with beta and conformable derivatives. Opt. Quant. Electron. **54**(11), 741 (2022)

Akram, G., Sadaf, M., Arshed, S., Sameen, F.: Traveling wave solutions of conformable time-fractional Klien–Fock–Gordon equation by the improved $\tan(\psi(\zeta)/2)$-expansion method. J. King Saud Univ. - Sci. **34**, 101822 (2022)

Akram, G., Sadaf, M., Zainab, I.: Effect of a new local derivative on space-time fractional nonlinear schrödinger equation and its stability analysis. Opt. Quant. Electron. **55**(9), 834 (2023)

Akram, G., Zainab, I.: Dark peakon, kink and periodic solutions of the nonlinear Biswas–Milovic equation with Kerr law nonlinearity. Optik **208**, 164420 (2020)

Aslan, I.: The discrete $(g'/g)$-expansion method applied to the differential-difference burgers equation and the relativistic Toda lattice system. Numer. Methods Part. Differ. Equ. **28**, 127–137 (2012). https://doi.org/10.1002/num.20611

Delkhosh, M., Cheraghian, H.: An efficient hybrid method to solve nonlinear differential equations in applied sciences. Comput. Appl. Math. **41**, 1–20 (2022). https://doi.org/10.1007/s40314-022-02024-9

Delkhosh, M., Parand, K.: Generalized pseudospectral method: theory and applications. J. Comput. Sci. **34**, 11–32 (2019)

Ghanbari, B., Günerhan, H., İlhan, O.A., Baskonus, H.M.: Some new families of exact solutions to a new extension of nonlinear Schrödinger equation. Physica Scripta **95**, 075208 (2020). https://doi.org/10.1088/1402-4896/ab8f42

Ghanbari, B., Inc, M.: A new generalized exponential rational function method to find exact special solutions for the resonance nonlinear schrödinger equation. Eur. Phys. J. Plus **133**, 1–18 (2018). https://doi.org/10.1140/epjp/i2018-11984-1

Ghanbari, B., Kuo, C.K.: New exact wave solutions of the variable-coefficient (1 + 1)-dimensional Benjamin–Bona–Mahony and (2 + 1)-dimensional asymmetric Nizhnik–Novikov–Veselov equations via the generalized exponential rational function method. Eur. Phys. J. Plus **134**, 1–13 (2019). https://doi.org/10.1140/epjp/i2019-12632-0

Houwe, A., Inc, M., Doka, S.Y., Acay, B., Hoan, L.V.: The discrete tanh method for solving the nonlinear differential-difference equations. Int. J. Mod. Phys. B **34**(7), 1 (2020). https://doi.org/10.1142/S0217979220501775

Modanli, M., Abdulazeez, S.T., Husien, A.M.: A residual power series method for solving pseudo hyperbolic partial differential equations with nonlocal conditions. Numer. Methods Part. Differ. Equ. **37**, 2235–2243 (2021). https://doi.org/10.1002/num.22683

Modanli, M., Murad, M.A.S., Abdulazeez, S.T.: A new computational method-based integral transform for solving time-fractional equation arises in electromagnetic waves. Zeitschrift fur Angewandte Mathematik und Physik **74**, 1–15 (2023). https://doi.org/10.1007/s00033-023-02076-9

Mohanty, S.K., Kravchenko, O.V., Dev, A.N.: Exact traveling wave solutions of the Schamel Burgers' equation by using generalized-improved and generalized $g'g$ expansion methods. Results Phys. **33**, 105124 (2022)

Parand, K., Delkhosh, M.: An efficient numerical solution of nonlinear Hunter–Saxton equation. Commun. Theoret. Phys. **67**(5), 483 (2017)

Parand, K., Moayeri, M.M., Latifi, S., Delkhosh, M.: A numerical investigation of the boundary layer flow of an Eyring–Powell fluid over a stretching sheet via rational Chebyshev functions. Eur. Phys. J. Plus **132**, 1–11 (2017). https://doi.org/10.1140/epjp/i2017-11600-0

Parand, K., Delkhosh, M., Nikarya, M.: Novel orthogonal functions for solving differential equations of arbitrary order. **10**, 31–55 (2017). https://doi.org/10.1515/tmj-2017-0004

Rasheed, S.K., Modanli, M., Abdulazeez, S.T.: Stability analysis and numerical implementation of the third-order fractional partial differential equation based on the caputo fractional derivative. J. Appl. Math. Comput. Mech. **22**(3), 1 (2023)

Sadaf, M., Akram, G.: Effects of fractional order derivative on the solution of time-fractional Cahn-Hilliard equation arising in digital image inpainting. Indian J. Phys. **95**, 891–899 (2021). https://doi.org/10.1007/s12648-020-01743-1

Sadaf, M., Akram, G., Dawood, M.: An investigation of fractional complex Ginzburg–Landau equation with Kerr law nonlinearity in the sense of conformable, beta and m-truncated derivatives. Opt. Quant. Electron. **54**, 1–22 (2022). https://doi.org/10.1007/s11082-022-03570-6

Sadaf, M., Arshed, S., Akram, G., Husaain, E.: Dynamical behavior of nonlinear cubic-quartic Fokas–Lenells equation with third and fourth order dispersion in optical pulse propagation. Opt. Quant. Electron. **55**, 1–14 (2023). https://doi.org/10.1007/s11082-023-05389-1

Tariq, H., Akram, G., Sadaf, M., Iftikhar, M., Guran, L.: Computational study for fiber Bragg gratings with dispersive reflectivity using fractional derivative. Fract. Fract. **7**, 625 (2023). https://doi.org/10.1088/1402-4896/ab8f42/meta

Tarla, S., Ali, K.K., Yilmazer, R., Osman, M.S.: Propagation of solitons for the Hamiltonian amplitude equation via an analytical technique. Mod. Phys. Lett. **36**, 7 (2022). https://doi.org/10.1142/S0217984922501202

Wang, H., Wen, X.Y.: Dynamics of dark multisoliton and rational solutions for three nonlinear differential-difference equations. Pramana **92**, 1–18 (2018). https://doi.org/10.1007/s12043-018-1671-5